

# Evolution of structure and microstructure of nanoperm nanocrystalline alloy with temperature

M. MIGLIERINI

Slovak University of Technology, Department of Nuclear Physics and Technology, Ilkovičova 3, 812 19 Bratislava, Slovakia

Effect of high temperature which influences nanocrystalline  $\text{Fe}_{90}\text{Zr}_7\text{B}_3$  NANOPERM alloy during Mössbauer effect examination is investigated.  $^{57}\text{Fe}$  Mössbauer spectroscopy was performed in temperature range from 25 to 800 °C upon a nanocrystalline alloy obtained from amorphous precursor by annealing at 515 °C for 1 hour. Using Mössbauer parameters obtained from high temperature (HT) spectra, development of structure and microstructure including dynamic processes is described as a function of temperature. Room temperature Mössbauer spectra collected after each HT experiment unveiled progressing crystallization and formation of new crystalline phases when the temperature of measurement has exceeded the onset of the first and the second crystallization step, respectively. Impact of multiple thermal treatments was studied upon sample annealed at 505 °C. Structural changes obtained after repeated annealing for 5 times 1 hour are compared with those after one 5-hour thermal treatment at the same temperature. Though the final stages of both heating scenarios are almost the same, the evolution of structure towards higher contents of nanocrystalline phase is observed after each repeated 1-hour annealing.

(Received September 5, 2006; accepted September 13, 2006)

**Keywords:** Mössbauer spectrometry, Nanocrystalline alloys, Temperature measurements

## 1. Introduction

Nanocrystalline alloys prepared by controlled annealing from rapidly quenched amorphous ribbons exhibit an interesting class of materials from the point of view of their magnetic properties [1]. Resulting magnetic parameters, which are superior to those of conventional transformer steels and/or amorphous materials, are ensured by a presence of crystalline grains several nanometres in size embedded in the amorphous residual phase [2]. Magnetic parameters of amorphous alloys are frequently deteriorated in the process of their practical employment by elevated temperature especially during prolonged operational times. On the other hand, nanocrystalline alloys are in fact already partially crystallized and from this point of view their structure is more resistant to such external effects and that is why it is more stable. Nevertheless, because the excellent magnetic behaviour of nanocrystalline alloys depends strongly on the amount and size of the crystalline grains, the mutual relation between microstructure and magnetic arrangement should be understood. Consequently, the effects of external conditions (*e.g.*, temperature) are frequently studied.

The effect of temperature upon structural arrangement as well as magnetic behaviour of nanocrystalline alloys is usually investigated from two viewpoints: (i) the effect of temperature of annealing [3, 4], and (ii) the effect of temperature of measurement [5-9]. The latter provides temperature dependencies of the parameters observed. The nature of nanocrystalline structure, which is established by controlled crystallization of amorphous precursors at certain annealing temperature, is sensitive to further temperature treatment that occurs, *e.g.* during *in situ*

temperature measurements. Because of this, the upper limit of measuring temperature is restricted to values well below (about 50 K) the onset of crystallization of the original amorphous precursor. Despite of this, temperature studies are very effective and the use of Mössbauer spectrometry, which allows identification of structurally and magnetically distinct regions within the sample, proved to be very useful [5].

Recently, a new approach was introduced [10] when Mössbauer spectrometry was used to follow the structural changes in  $\text{Fe}_{90}\text{Zr}_7\text{B}_3$  exposed to *in situ* high temperatures extended even behind the second crystallization stage. The sample was “precrystallized” at the end of the first crystallization stage at 620 °C for 1 hour exhibiting optimal magnetic properties. These were ensured by relatively high relative fraction of bcc-Fe nanocrystals (ca. 67%).

In this work, the same  $\text{Fe}_{90}\text{Zr}_7\text{B}_3$  NANOPERM alloy is investigated. However, we concentrate on samples with low crystalline fraction which were prepared by thermal treatments at temperatures close to the onset of crystallization. The structure is at the early stage of its transformation and, thus, more sensitive to further changes induced by temperature. Mössbauer spectrometry performed at temperatures up to 800 °C (*i.e.*, behind the Curie point of bcc-Fe) was chosen as a principal method of investigation.

## 2. Experimental

Amorphous precursors of the nominal composition of  $\text{Fe}_{90}\text{Zr}_7\text{B}_3$  were prepared by melt-spinning technique in a protective atmosphere. The resulting ribbons were 21(1)

$\mu\text{m}$  thick and 15 mm wide. The amorphous state of the starting material was evidenced by Mössbauer spectroscopy at room temperature [10].

Differential scanning calorimetry (DSC) in Fig. 1a shows the evolution of structure with temperature. Characteristic temperatures of the onset of the first and the second crystallization steps  $T_{x1}$  and  $T_{x2}$ , respectively, are marked with arrows. It should be noted that the DSC was taken by the rate of 10K/min. Using the results of DSC, three types of nanocrystalline samples were prepared: Sample (A) was annealed at the beginning of the first crystallization stage at 515 °C for 1 hour. Sample (B) was annealed at the onset of crystallization at 505 °C for 1 hour. This thermal treatment was repeated five times. After each annealing, a Mössbauer spectrum was recorded. Sample (C) was heat treated at 505 °C for 5 hours. Annealing was performed under high vacuum conditions.

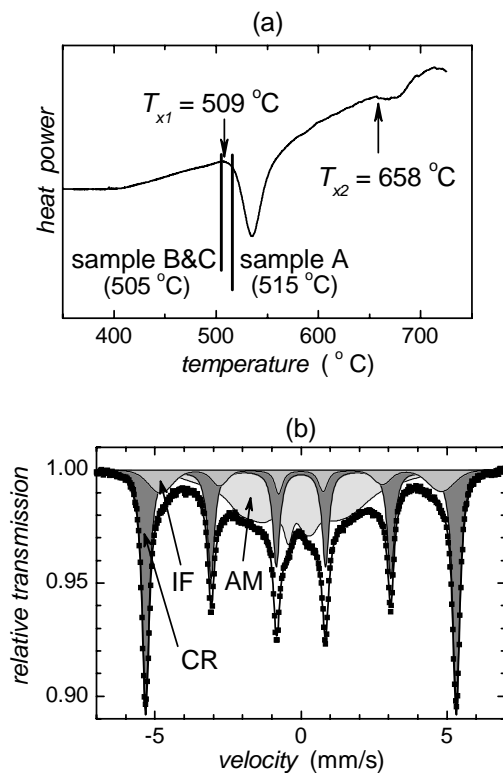


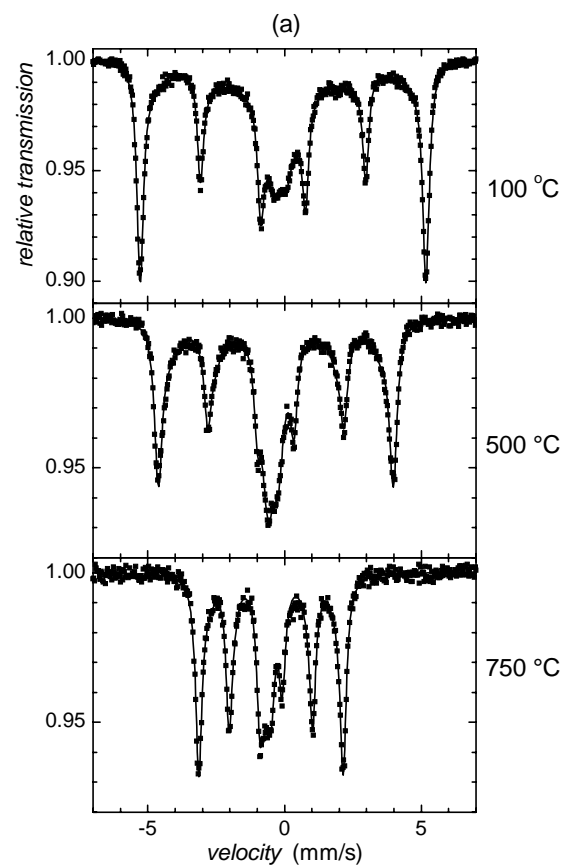
Fig. 1. DSC (a) and RT Mössbauer spectrum of nanocrystalline  $\text{Fe}_{90}\text{Zr}_7\text{B}_3$  with its components (b).

Mössbauer spectra were recorded at different temperatures ranging from room temperature (RT) up to 800 °C using a  $^{57}\text{Co}(\text{Rh})$  source. Temperature experiments were performed in a commercial vacuum furnace attached to a constant acceleration Mössbauer spectrometer. After every high temperature (HT) experiment, the sample was cooled down to RT and Mössbauer spectrum was collected in order to monitor the state of the sample. All spectra were recorded with the sample placed inside the furnace thus ensuring the same geometrical conditions for both HT and RT Mössbauer experiments. HT and RT spectra were taken for about 8 hours each.

Hyperfine parameters of Mössbauer spectra were refined using the Confit evaluation software [11]. Isomer shift (IS) values are quoted with respect to RT Mössbauer spectrum of  $\alpha\text{-Fe}$  calibration foil. In the fitting model, amorphous residual matrix (AM), interface regions (IF), and crystalline phases (CR) were considered [12, 13]. The latter were reconstructed by the help of narrow Lorentzian components whereas AM and IF subspectra were fitted by distributions of hyperfine parameters. RT Mössbauer spectrum of nanocrystalline sample A is shown in Fig. 1b together with its spectral components.

### 3. Results

Typical examples of HT and RT Mössbauer spectra taken after HT experiments of sample A are shown in Fig. 2a and 2b, respectively. In general, the spectra consist of narrow lines which are superimposed upon central broad feature (see also Fig. 1b). The former represent crystalline phase (CR) whereas the latter is assigned to amorphous residual matrix (AM). Between the two, interface regions (IF) can be identified. They comprise atoms located on the surface of nanocrystalline grains and those atoms of AM which are in close contact with them. IF component is demonstrated in Mössbauer spectra as a shoulder in the inner part of the first and/or sixth narrow CR lines as seen in Fig. 1b.



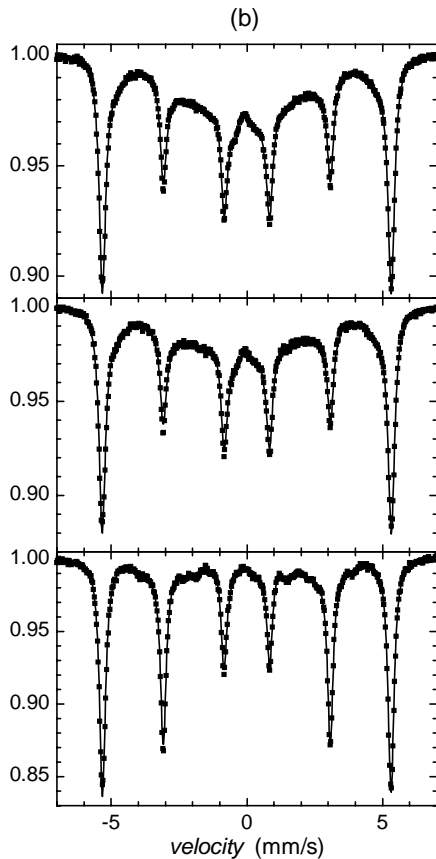


Fig. 2. Mössbauer spectra of nanocrystalline  $Fe_{90}Zr_7B_3$  alloy annealed at  $515\text{ }^{\circ}\text{C}/1\text{h}$  (sample A) which were taken at the indicated temperatures (a) and at RT after the indicated temperatures (b).

The effect of temperature of measurement on HT Mössbauer spectra in Fig. 2a is demonstrated by noticeable narrowing of a whole spectrum and continuous evolution of the central part of spectra with rising temperature. Both effects are associated with changes in the magnetic microstructure.

RT Mössbauer spectra in Fig. 2b provide comparison of structural changes which took place in the investigated samples during HT experiments. An apparent vanishing of the broad central part in Mössbauer spectra is due to progressing crystallization process during HT experiments which leads to decrease in AM and IF on account of CR.

The disappearance of the IF component is demonstrated in Fig. 3 where Mössbauer spectra taken at RT before and after HT experiment at  $700\text{ }^{\circ}\text{C}$  are compared. The inset clearly shows that the IF component is not present in the Mössbauer spectrum taken after the HT experiment. This can be considered as an indirect proof in favour of the concept of interfacial regions [12, 14]. Should the IF component be due to Zr or B inclusions in the bcc-Fe lattice [8, 9], one would expect that their incorporation into Fe matrix will be even more pronounced during high temperature measurements when the crystallization takes place.

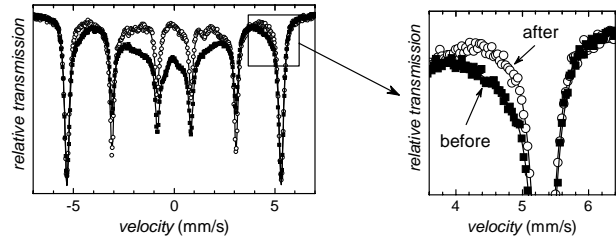


Fig. 3. RT Mössbauer spectra of nanocrystalline  $Fe_{90}Zr_7B_3$  alloy (sample A) taken before (solid squares) and after measurement at  $700\text{ }^{\circ}\text{C}$  (open circles).

Mössbauer spectra of sample B annealed for 1 hr. and 5-times for 1 hr. are compared in Fig. 4a. Changes in the central part of the spectra are related to progressing crystallization during the repetitive annealing.  $A_{CR}$  in Fig. 4b shows slow but sure increase with the number of thermal treatments on account of decreasing  $A_{AM}$  contribution. IF does not exhibit any appreciable modifications within the range of experimental error. This means that the size of crystalline grains does not change. Hyperfine magnetic fields  $B_f$  and isomer shift values  $IS_f$  ( $f = AM, IF, CR$ ) are not affected by repeated thermal treatments.

Sample C, which was treated at  $505\text{ }^{\circ}\text{C}$  for 5 hrs, exhibits almost the same Mössbauer spectrum as sample B after 5-fold one-hour annealing. All Mössbauer parameters of both samples coincide within the experimental error. For comparison, relative fractions of individual spectral components of sample C are plotted in Fig. 4b by asterisks.

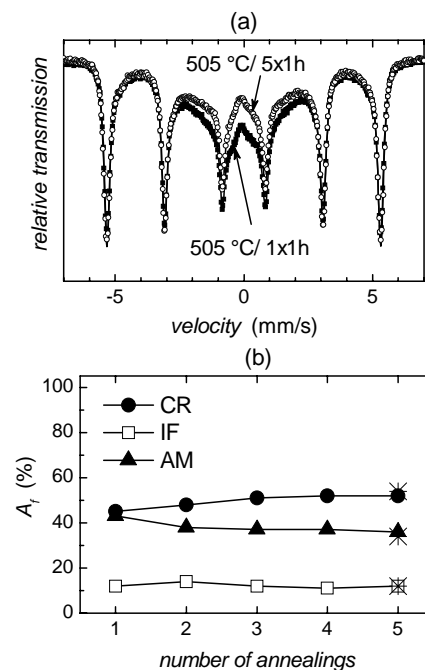


Fig. 4. RT Mössbauer spectra of nanocrystalline  $Fe_{90}Zr_7B_3$  alloy annealed at  $505\text{ }^{\circ}\text{C}$  (sample B) for 1 hr. (solid squares) and repeatedly 5-times 1 hr. (open circles) (a) and relative fraction  $A_f$  ( $f = AM, CR, IF$ ) (b) derived from Mössbauer spectra of samples after multiple annealing for 1 hr. Asterisks represent parameters of sample C.

#### 4. Discussion

Evolution of hyperfine parameters with temperature of measurement and at RT after HT experiments is presented in Fig. 5a and 5b, respectively. Dashed vertical lines denote temperatures of the onset of the first  $T_{x1}$  and the second  $T_{x2}$  crystallization steps. Quantitative features are summarized by the help of temperature dependences of hyperfine fields  $B_f$ , isomer shifts  $IS_f$ , and relative fractions  $A_f$ .

$B_{CR}$  and  $IS_{CR}$  displayed in Fig. 5 represent hyperfine parameters of only the principal crystalline phase present in the nanocrystalline  $Fe_{90}Zr_7B_3$  alloy which was identified as bcc-Fe. For comparison, data of a bulk calibration Fe foil are plotted by dotted lines. As seen, no appreciable deviations in hyperfine parameters of bulk and nanocrystalline Fe grains are observed for either HT or RT experiments. Temperature decrease of  $B_{CR}$  and  $IS_{CR}$  in Fig. 5a follows the expected behaviour.  $B_{CR}$  drops to zero at 770 °C which is a Curie temperature of bcc-Fe [15]. No deviations in  $B_{CR}$  and  $IS_{CR}$  in Fig. 5b indicate that the principal crystalline phase in samples cooled down to RT after HT experiments is stable from a crystallographic point of view.

It is noteworthy that in the temperature region where the IF component is present in the samples, the  $B_{IF}$ - and  $IS_{IF}$ -values follow the same tendency and/or are almost identical with the corresponding parameters of a bcc-Fe phase. Consequently, from a structural point of view a close similarity between resonant atoms located in CR and IF is confirmed. This supports the assumption that IF atoms belong to nanocrystalline grains and deviation in  $B_{IF}$  is due to broken symmetry on the surface of nanograins [14].

The development of relative fraction  $A_{CR}$  during (Fig. 5a) and after (Fig. 5b) HT Mössbauer effect measurements takes into consideration also formation of other crystalline phases which emerged in the investigated sample at temperatures higher than 600 °C. The measured magnetic hyperfine fields appear in the range 17.6-20.8 T, 20.8-22.7 T, and 23.5-24.7 T with relative contribution of 12-18 %. They are close to those reported for  $Fe_2Zr$  and  $Fe_3Zr$  [16, 17]. The difference in the increase of  $A_{CR}$  observed in Fig. 5b goes on the account of the principal bcc-Fe grains which grow both in number and also in size. As a result, the relative contribution of surface atoms decreases and the corresponding IF component eventually vanishes after measurements at temperatures higher than 600 °C.

The progressing crystallization during Mössbauer effect measurements at elevated temperatures is observed in HT spectra by a rapid increase in  $A_{CR}$  as seen in Fig. 5a. In addition, grain growth of bcc-Fe crystals effectively decreases the contribution of surface atoms. Consequently, the IF component in HT spectra completely vanishes already at 500 °C.

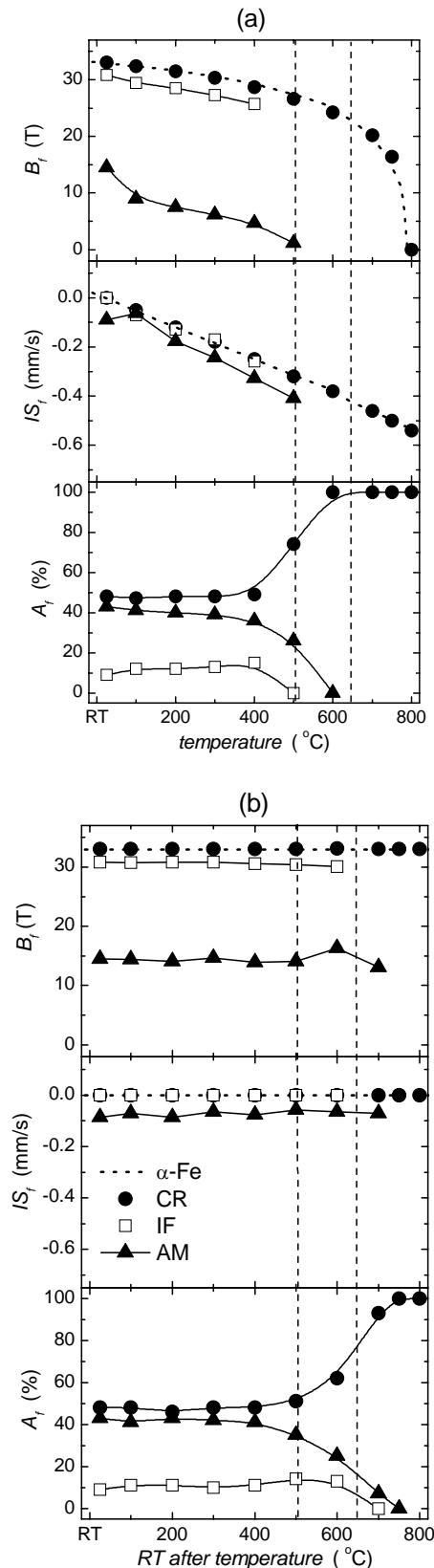


Fig. 5. Hyperfine magnetic field  $B_f$ , isomer shift  $IS_f$ , and relative fraction  $A_f$  ( $f = AM, IF, CR$ ) of  $Fe_{90}Zr_7B_3$  as derived from (a) HT and (b) RT Mössbauer spectra.

Transformation of AM into CR (bcc-Fe +  $Fe_2Zr$ ,  $Fe_3Zr$ ) is illustrated by changes in the central part of the

Mössbauer spectra in Fig. 3 and 4a. Formation of crystalline grains introduces stresses which affect through magnetostriction the orientation of magnetic moments. As a result, the net magnetization tends to turn into the plane of the ribbon-shaped sample which is demonstrated by enhanced intensity of the second and fifth lines.

## 5. Conclusions

Influence of high temperature on structure and magnetic microstructure of nanocrystalline  $\text{Fe}_{90}\text{Zr}_7\text{B}_3$  alloy were investigated by the help of “*in situ*” high temperature and “*ex post*” room temperature Mössbauer effect experiments.

The evolution of hyperfine parameters in sample A has revealed similar trends as those reported in [10]. Nevertheless, due to lower crystalline fraction in the present samples the onset of crystallization induced during HT Mössbauer effect experiments is revealed at lower measuring temperature but exhibits more evident progress. Thus, inferior structural stability of nanocrystalline alloy with lower crystalline contents can be deduced.

Comparison of samples B and C did not unveil any differences in spectral parameters obtained after 5-fold one-hour exposures to 505 °C and a single annealing for 5 hours. However, a gradual increase in relative contents of crystalline phase is observed as a function of number of thermal treatments for 1 hour.

## Acknowledgement

This work was supported by Science and Technology Assistance Agency under the contract No. APVT-20-008404. Discussions with J. M. Grenèche are acknowledged.

## References

- [1] K. Suzuki, A. Makino, A. Inoue, T. Masumoto, J. Appl. Phys. **70**, 6232 (1991).
- [2] G. Herzer, Phys. Scr., **T49**, 307 (1993).
- [3] M. Kopcewicz, A. Grabias, D. L. Williamson, J. Appl. Phys. **82**, 1747 (1997).
- [4] S. H. Yoon, S. B. Kim, H. M. Lee, Ch. S. Kim, J. Magn. Magn. Mat. **507**, 254 (2003).
- [5] A. Slawska-Waniewska, J.-M. Grenèche, Phys. Rev. B, **9**, R8491 (1997).
- [6] M. Miglierini, J. M. Grenèche, J. Phys.: Condens. Matter **15**, 5637 (2003).
- [7] K. Suzuki K., J. M. Cadogan, Phys. Rev. B, **58**, 2730 (1998).
- [8] J. Balogh, L. Bujdosó, D. Kaptás, T. Kemény, I. Vincze, S. Szabó, D. L. Beke, Phys. Rev. B **61**, 4109 (2000).
- [9] T. Kemény, D. Kaptás, L. F. Kiss, J. Balogh, I. Vincze, S. Szabó, D. L. Beke, Hyperfine Interact., **130**, 181 (2000).
- [10] S. Stankov, B. Sepiol, T. Kanuch, D. Scherjau, R. Würschum, M. Miglierini, J. Phys.: Condens. Matter **17**, 3183 (2005).
- [11] J. Kučera, V. Veselý, T. Žák: 1986-2005 Mössbauer Spectra Convolution Fit for Windows 98/2K/XP, ver. 4.191.
- [12] M. Miglierini, J. M. Grenèche, J. Phys.: Condens. Matter **9**, 2303 (1997).
- [13] M. Miglierini, J. M. Grenèche, J. Phys.: Condens. Matter **9**, 2321 (1997).
- [14] J. M. Grenèche, A. Slawska-Waniewska, J. Magn. Magn. Mat., **215-216**, 264 (2000).
- [15] R. S. Preston, S. S. Hanna, J. Heberle, Phys. Rev. **168**, 2207 (1962).
- [16] A. K. Zhubaev, A. B. Argynov, K. K. Kadyrzhanov, V. S. Rusakov, T. E. Turkebaev, Proc. 8<sup>th</sup> Int. Conf. Solid State Physics, Almaty, Ed. K. K. Kadyrzhanov, TOO Print-S, Almaty, Kazakhstan, 2005, ISBN 9965-675-18-X, Vol. I. p. 338.
- [17] G. Concas, F. Congiu, G. Spano, M. Bionducci, J. Magn. Magn. Mat. **279**, 421 (2004).

\*Corresponding author: bruno@eff.stuba.sk